Development and Analysis of a Modified Saleh-Valenzuela Channel Model for the UHF Band

Artur Nalobin, Sven Dortmund, Sebastian Sczyslo,
Jan Barowski, Bastian Meiners and Ilona Rolfes
Ruhr-Universität Bochum, Bochum, Germany

***Abstract*—This contribution deals with the analysis of a modified Saleh-Valenzuela channel model for the UHF band. The development of the channel model is based on indoor channel measurements within a large exhibition hall in a line-of-sight scenario in order to study new cognitive radio systems. Contrary to the conventional modeling, the path voltage gain is modeled by a Rayleigh probability density function. Due to the broad-band consideration the channel model can be used for a variety of different operating frequencies.**

I. Introduction

Programme Making and Special Event applications (PMSE) are commonly operated in large concert and exhibition halls to transmit high quality audio and video data. Due to the reallocation of the frequency spectrum by the Digital Dividend and the higher user density, PMSE devices have a strongly decreasing frequency range available in which they can operate. Furthermore, PMSE systems are predominantly used in indoor scenarios. In this case the radio channel is strongly influenced by the high amount of multipath components (MPCs) of the transmitted signal. The result is a highly probable destructive signal interference, particularly for PMSE applications due to their typically narrow bandwidth. To improve the frequency utilization and the coexistence of PMSE systems with broadcast channels a dynamic frequency access concept as provided by a cognitive radio system and the usage of alternative operation frequencies preferable in the UHF band is of interest [1]. In order to develop new concepts by means of a simulation environment, a realistic channel model is of interest. This model has to represent the channel accurately with its site specific fading characteristics for a variety of operating frequencies.

Most existing models for the characterization of channel parameters in the UHF range were predominantly developed with respect to the radio network planning of mobile telecommunication services. The investigations in this paper deal with a statistical channel model for mobile devices used in indoor and line-of-sight (LOS) scenarios. Although the channel model is derived primarily for narrow-band PMSE devices, it can be used for diverse narrow as well as broad-band systems. The model is based on the Saleh-Valenzuela (SV) cluster model for the simulation of a channel impulse response (CIR) [2]. The analysis is based on a measurement campaign performed in a large exhibition hall in Berlin, Germany, within the frequency range from $0.3\,\mathrm{GHz}$ to $3\,\mathrm{GHz}$. The conventional SV model is rest upon the assumption that the average path power decreases exponentially within every cluster of rays. This paper shows an approach using the Rayleigh distribution for the average power of the paths within a cluster. To realize a suitable clustering procedure a deconvolution process was applied to the measurement data.

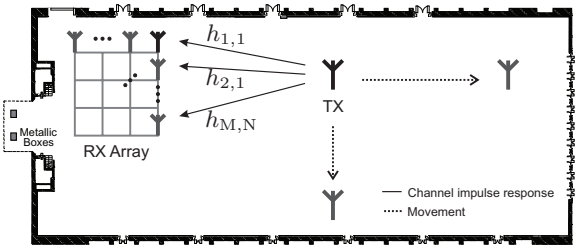

Fig. 1. A plain overview of the measurement environment and configuration with one transmit and 121 receive antennas for one of 170 large-scale positions.

To analyze the new approach in more detail the paper is structured as follows. In section II the measurement campaign including the setup and equipment as well as the deconvolution of the CIRs are explained briefly. Section III reviews the theoretical background of the conventional and the modified SV cluster model including the clustering procedure. Section IV presents the channel parameter statistics followed by the conclusion in section V.

II. Measurement Campaign and Signal Processing

A. Measurement Campaign in the UHF Band

The channel characteristics in a LOS scenario are derived from a measurement campaign in the fairground of Berlin, Germany. Here, the campaign was performed within the frequency range from $0.3\,\mathrm{GHz}$ to $3\,\mathrm{GHz}$ using a vector network analyzer. The measurement setup and equipment are described in detail in [3].

Essentially, the measurement setup can be subdivided into two parts. The first part is a large-scale setup to incorporate local differences. The position of the transmit and the receive antenna was locally varied within the hall with a distance d from $5\,\mathrm{m}$ to $80\,\mathrm{m}$ and 170 large-scale positions altogether. The second part is a small scale setup to cover local variations in the vicinity of a measurement position. It is realized by a virtual array for the positioning of the receive antenna on a $1\,\mathrm{m} \times 1\,\mathrm{m}$ rectangular grid with 121 measurement positions. An overview of the hall including the measurement setup and indicated movement of the antennas is depicted in Fig. 1.

B. Iterative Deconvolution of the CIR

Due to the finite bandwidth, the power delay profile (PDP) $h_{\mathrm{meas}}(t)$ measured in II-A is not an ideal complex-valued filter with an finite impulse response (FIR). Therefore $h_{\mathrm{meas}}(t)$ does not correspond to a weighted summation of Dirac impulses [4].

ISBN 978-3-9812668-6-3

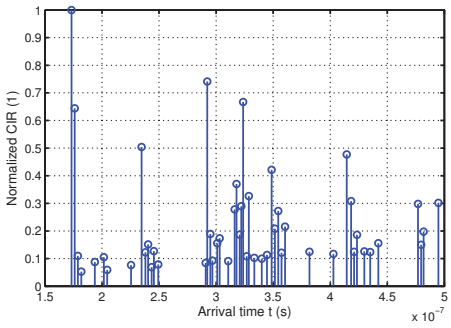

Fig. 2. A sample of a normalized $|h_{\mathrm{CIR}}(t)|$ according to the distance of 50 m.

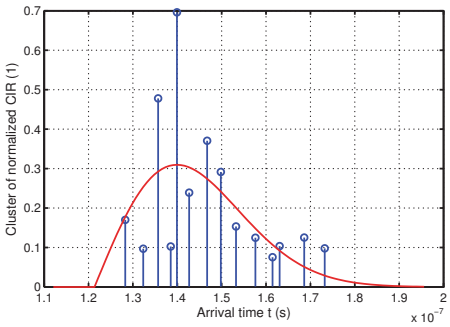

Fig. 3. Sample cluster with paths (○) from a CIR matched by a function with a Rayleigh shape (–) according to the distance of 20 m.

Neglecting noise and pulse distortion, $h_{\mathrm{meas}}(t)$ consists of a superposition of the template functions $p(t)$ weighted by the complex-valued factor β_m and time shifted by τ_m:

$$\begin{aligned} h_{\mathrm{meas}}(t) &= \sum_{l} \beta_l \delta(t-\tau_l) * p(t) \\ &= h_{\mathrm{CIR}}(t) * p(t) \end{aligned} \tag{1}$$

Based on this assumption, the CLEAN algorithm, known from radio astronomy, was used to calculate the complex-valued factors β_l and the time shifts τ_l of the ideal impulse response $h_{\mathrm{CIR}}(t)$ in (1) [5]. Basically, the CLEAN algorithm performs iteratively a subtractive deconvolution of $h_{\mathrm{meas}}(t)$ in the time domain. Fig. 2 shows a sample of the impulse response $h_{\mathrm{CIR}}(t)$ extracted by the CLEAN algorithm.

III. Theoretical Background of the Saleh-Valenzuela Channel Model

A. Conventional SV Channel Model

The SV channel model is based on the assumption that the multipath components of the transmitted signal are received in clusters due to multiple reflections from objects and is described in detail in [2]. With the amplitude $\beta_{r,m}$ and the phase $\theta_{r,m}$ of the r-th path in the m-th cluster, the equivalent channel impulse response is modeled as

$$h_{\mathrm{CIR}}(t) = \sum_{m=0}^{M} \sum_{r=0}^{R} \beta_{\mathrm{r,m}} \mathrm{e}^{\mathrm{j}\theta_{\mathrm{r,m}}} \delta(t - T_m - \tau_{r,m}). \tag{2}$$

In (2) T_m is the arrival time of the m-th cluster and $\tau_{r,m}$ describes the arrival time of the r-th path inside the m-th cluster, with generally the number of paths $R \to \infty$ and the number of cluster $M \to \infty$. Further, $\theta_{\mathrm{r,m}}$ is modeled as uniformly distributed over $[0, 2\pi)$ and $\beta_{\mathrm{r,m}}$ follows the Rayleigh distribution with

$$p(\beta_{r,m}) = 2\,\beta_{r,m}/\overline{\beta_{r,m}^2}\,\mathrm{e}^{-\beta_{r,m}/\overline{\beta_{r,m}^2}}. \tag{3}$$

In (3) $\overline{\beta_{r,m}^2}$ corresponds to the average power of the r-th path inside the m-th cluster and decreases exponentially on both the entire CIR as well as within each cluster.

The arrival times of the rays $\tau_{r,m}$ and of the clusters T_m are described by Poisson processes of different arrival rates. According to the model, the inter-arrival exponential probability density functions (PDF) of T_m with an average arrival rate Λ and of $\tau_{r,m}$ with an average arrival rate λ are equal to

$$p(T_m, T_{m-1}) = \Lambda\, e^{-\Lambda(T_m - T_{m-1})}, \quad m \in \mathbb{N}^+, \tag{4}$$

$$p(\tau_{r,m}, \tau_{(r-1),m}) = \lambda\, e^{-\lambda(\tau_{r,m} - \tau_{(r-1),m})}, \quad r \in \mathbb{N}^+. \tag{5}$$

B. Modified SV Channel Model with Rayleigh Clusters

Considering deconvoluted CIRs by means of the CLEAN algorithm in section II-B it can be stated that the exponential decay of the average signal power inside the clusters does not match the measured data. For illustration Fig. 3 shows the extracted paths of one representative sample cluster. It seems that the shape of the paths follow tendentially a shape which is comparable to the Rayleigh distribution [6], instead of an exponential decay. Here, the Rayleigh distribution is chosen due to its simplicity even if other functions with similar favorable behavior may exist.

On the basis of this experience and expertise the channel modeling of the CIR in this contribution relies on the SV channel model with the extension that the rays within one cluster follow the shape of the Rayleigh distribution. This assumption is valid for all clusters except the first cluster, which decays due to the LOS path exponentially with the arrival time. Assuming Rayleigh distribution for the characterization of the probability density function, the Rayleigh matching for the clusters is described with the following function

$$f(t, \sigma, \gamma, \tau) = \begin{cases} \gamma \cdot \frac{(t-\tau)\, e^{-\frac{(t-\tau)^2}{2\sigma^2}}}{\sigma^2} & , t \geq 0 \\ 0 & , t < 0 \end{cases} \tag{6}$$

In this case $f(t, \sigma, \gamma, \tau)$ is the average of the normalized amplitude of the CIR distributed with the PDF in (3). Further, the time t is equal to the arrival time normalized to the LOS path. The factors γ and τ in (6) allow to determine the location and the scaling of $f(t, \sigma, \gamma, \tau)$. In general, the shape of the Rayleigh distribution is described by the single parameter σ, which influences particularly the "width" of the function. Whereby, the maximum of (6) is located at $t_c = \sigma + \tau$ and is referred in the following as the centroid of a cluster.

C. Clustering Procedure of MPCs

For the modeling approach, considered in this contribution, a clustering procedure of the MPCs of the impulse response h_{CIR} is necessary. In the sample CIR in Fig. 2 it is already possible to make visually sufficiently precise clusters. For a

ISBN 978-3-9812668-6-3

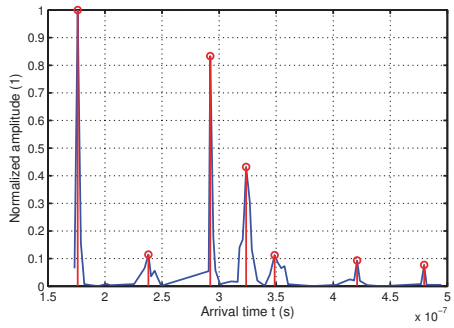

Fig. 4. Normalized $|\ddot{h}_{\mathrm{CIR}}(t)|$ of a sample CIR (–) with local maxima (○) indicating centroids according to the distance of 50 m.

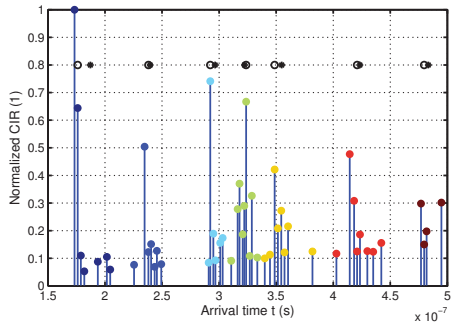

Fig. 5. Clustering of a sample impulse response $h_{\mathrm{CIR}}(t)$ (different color per cluster) with indicated centroids derived from $|\ddot{h}_{\mathrm{CIR}}(t)|$ (○) and from the k-means algorithm (∗) according to the distance of 50 m.

simple and reliable analysis the k-means algorithm was used [7]. This algorithm forms similar values to a predefined number of k clusters. The disadvantage relies on the fact, that the number of the clusters and the individual starting values of these clusters must be known.

Due to the assumptions, that both T_m and $\tau_{r,m}$ follow the inter-arrival exponential PDFs in (4) and (5) and that the amplitude decay can be described by the Rayleigh distribution, the differential calculus of the $h_{\mathrm{CIR}}(t)$ is used to calculate the required number and positions of the initial centroids. The first differential applied to the impulse response $h_{\mathrm{CIR}}(t)$ in (1) is as follows

$$\dot{h}_{\mathrm{CIR}}(t) = \mathfrak{D}\left\{h_{\mathrm{CIR}}(t)\right\} = \frac{\beta_{l+1} - \beta_l}{\tau_{l+1} - \tau_l}, \tag{7}$$

whereby $\ddot{h}_{\mathrm{CIR}}(t) = \mathfrak{D}\left\{\dot{h}_{\mathrm{CIR}}(t)\right\}$, and increases tendentially for large amplitude differences $\beta_{l+1} - \beta_l$ and small inter-arrival delays $\tau_{l+1} - \tau_l$ between adjacent rays. Through this approach the characteristics of the clusters are exploited to indicate the number and positions of centroids by choosing local maxima of $|\ddot{h}_{\mathrm{CIR}}(t)|$. Using this procedure Fig. 4 shows the magnitude of the normalized $|\ddot{h}_{\mathrm{CIR}}(t)|$ of the CIR with seven estimated centroids. This figure shows a clear correlation between the position of the local maxima and possible clusters in Fig. 2. Applying this approach and the k-means algorithm to a sample CIR, the result can be seen in Fig. 5. The applied clustering procedure shows a clear and intuitive approximation of the clusters.

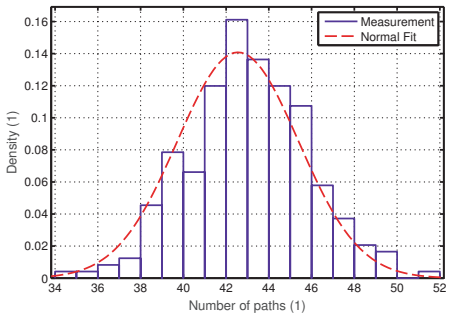

Fig. 6. Probability density function of the number of paths deconvoluted from all CIRs with a distance of 80 m.

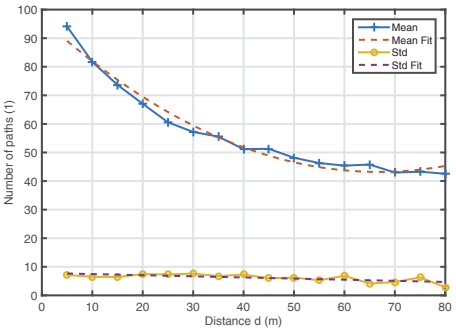

Fig. 7. Mean and standard deviation of the number of paths deconvoluted from all CIRs as a function of the distance.

IV. Site-specific Channel Parameter Statistics

In this section necessary parameters and their statistics will be considered in more detail to derive the modified SV channel model. The investigations show that the parameters generally depend on the distance between the transmitter and receiver within the exhibition hall.

A. Statistical Parameterization of the Paths

The total number of the extracted paths can be approximated statistically by the normal distribution, whose probability density function (PDF) can be seen in Fig. 6 for the CIRs with the distance $d = 80\,\mathrm{m}$. In Fig. 7 the total number of the paths of all deconvoluted CIRs as a function of the distance d between 5 m and 80 m including a polynomial curve fitting by least squares is depicted. Here, the deconvoluted CIRs include not only the most significant paths, but rather also paths with small amplitudes and therefore paths with a low energy content. While the standard deviation is with approximately 7 paths nearly constant, there is a significant distance dependence of the mean value, which decays from 94 paths at the distance of 5 m to 42 paths at 80 m. It should be noted that Fig. 7

Fig. 8 shows the mean and standard deviation of the total number of clusters derived from all CIRs in dependence on the distance. The parameters show a similar behavior as the number of paths in Fig. 7. While the standard deviation is nearly constant between 1 and 1.5 clusters, there is a distance dependence on the mean value, which decays from 10 clusters at 5 m to approximately 6 clusters at 80 m.

Since the first cluster with the LOS path in the modified model is assumed to decay exponentially, this cluster is modeled separately for the remaining clusters. Fig. 9 shows the

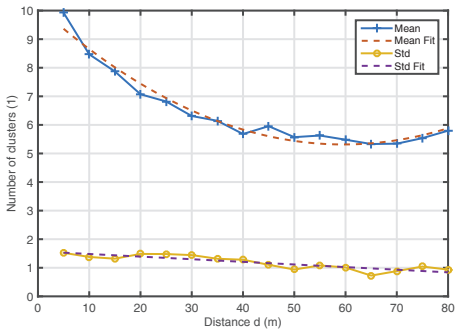

Fig. 8. Mean and standard deviation of the number of clusters derived from all CIRs as a function of the distance.

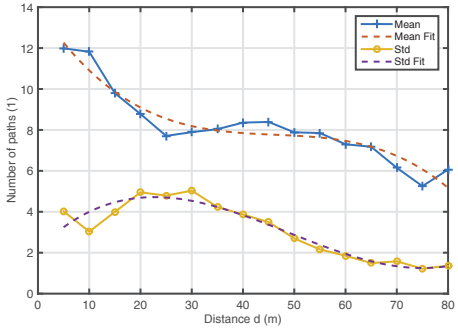

Fig. 9. Mean and standard deviation of the number of paths within the first cluster deconvoluted from all CIRs as a function of the distance.

statistical behavior of the number of the paths within the first cluster.

The number of paths within the remaining clusters can be described with the normal distribution and is nearly constant. The relative arrival time of the centroids (arrival time of centroid subtracting arrival time of LOS path) can be approximated by the Weibull distribution (with scale parameter a and shape parameter b) and the time between adjacent paths within clusters follows the log-normal distribution. The modeled parameters and the coefficients derived from polynomial fitting using least-squares approximation are listed in Table I.

The analysis of the Rayleigh factor σ in (6) show that this parameter can be approximated by the log-normal distribution and is nearly independent on the distance. In Fig. 10 a sample of the Rayleigh factor for the distance of $5\,\mathrm{m}$ is depicted. It is obvious that the rayleigh factor is dependent on the arrival time of the centroids. For illustration the figure contains the linear regression with $\sigma \approx 28.80 \times 10^{-3}\ \frac{1}{\mathrm{s}} \times T + 9.44 \times 10^{-9}$, here, T is the relative arrival time of the centroids.

V. Conclusion

The concept of the modified Saleh-Valenzuela Channel Model was explained including its relevance for the development and analysis of new radio systems. While the conventional assumption of exponential decay of the path amplitudes represents a good approximation, within the measurements it could be observed that the average power of the paths within a cluster can be described more accurately by the Rayleigh distribution. Measurement results within a large exhibition hall show a dependency of the statistical parameters on the distance. Main characteristics of the channel model are described and presented with its statistics.

TABLE I. Polynomial function coefficients of the fitted distribution functions of all deconvoluted CIRs dependent on the distance

Parameter	Distribution	Polynomial Coefficients
Total number of paths	Normal $\mu = \mu_0 + \mu_1 d + \mu_2 d^2$ $\sigma = \sigma_0 + \sigma_1 d$	$\mu_0 = 96.78$ $\mu_1 = -1.60\ \frac{1}{\mathrm{m}}$ $\mu_2 = 12.01 \times 10^{-3}\ \frac{1}{\mathrm{m}^2}$ $\sigma_0 = 7.8452$ $\sigma_1 = -39.39 \times 10^{-3}\ \frac{1}{\mathrm{m}}$
Total number of clusters	Normal $\mu = \mu_0 + \mu_1 d + \mu_2 d^2$ $\sigma = \sigma_0 + \sigma_1 d$	$\mu_0 = 10.14$ $\mu_1 = -0.16\ \frac{1}{\mathrm{m}}$ $\mu_2 = 1.36 \times 10^{-3}\ \frac{1}{\mathrm{m}^2}$ $\sigma_0 = 1.57$ $\sigma_1 = -9.17 \times 10^{-3}\ \frac{1}{\mathrm{m}}$
Number of paths within the first cluster	Normal $\mu = \mu_0 + \mu_1 d + \mu_2 d^2 + \mu_3 d^3$ $\sigma = \sigma_0 + \sigma_1 d + \sigma_2 d^2 + \sigma_3 d^3$	$\mu_0 = 13.98$ $\mu_1 = -0.38\ \frac{1}{\mathrm{m}}$ $\mu_2 = 8.01 \times 10^{-3}\ \frac{1}{\mathrm{m}^2}$ $\mu_3 = -57.79 \times 10^{-6}\ \frac{1}{\mathrm{m}^3}$ $\sigma_0 = 2.17$ $\sigma_1 = 0.25\ \frac{1}{\mathrm{m}}$ $\sigma_2 = -7.12 \times 10^{-3}\ \frac{1}{\mathrm{m}^2}$ $\sigma_3 = 48.60 \times 10^{-6}\ \frac{1}{\mathrm{m}^3}$
Number of paths within clusters except the first cluster	Normal $\mu = \mu_0 + \mu_1 d$ $\sigma = \sigma_0 + \sigma_1 d$	$\mu_0 = 8.35$ $\mu_1 = 3.07 \times 10^{-3}\ \frac{1}{\mathrm{m}}$ $\sigma_0 = 2.43$ $\sigma_1 = -4.76 \times 10^{-3}\ \frac{1}{\mathrm{m}}$
Relative arrival time of centroids	Weibull $a = a_0 + a_1 d$ $b = b_0 + b_1 d$	$a_0 = 2.41 \times 10^{-7}\ \mathrm{s}$ $a_1 = -1.30 \times 10^{-9}\ \frac{\mathrm{s}}{\mathrm{m}}$ $b_0 = 1.68$ $b_1 = 12.63 \times 10^{-3}\ \frac{1}{\mathrm{m}}$
Time between adjacent paths within clusters	Log-Normal $\mu = \mu_0 + \mu_1 d$ $\sigma = \sigma_0 + \sigma_1 d$	$\mu_0 = -19.44\ \ln(\mathrm{s})$ $\mu_1 = -0.72 \times 10^{-3}\ \frac{\ln(\mathrm{s})}{\mathrm{m}}$ $\sigma_0 = 0.63$ $\sigma_1 = -0.54 \times 10^{-3}\ \frac{1}{\mathrm{m}}$

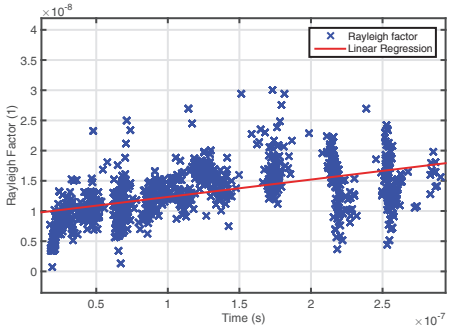

Fig. 10. Rayleigh factor in dependence on the arrival time of the centroids for the distance of $5\,\mathrm{m}$.

References

[1] J. Brendel, S. Riess, A. Stoeckle, R. Rummel, and G. Fischer, "A spectrum sensing network for cognitive pmse systems," *Frequenz Journal of RF-Engineering and Telecommunications*, 2012.

[2] A. Saleh and R. Valenzuela, "A statistical model for indoor multipath propagation," *Selected Areas in Communications, IEEE Journal on*, vol. 5, no. 2, pp. 128–137, February 1987.

[3] S. Sczyslo, S. Dortmund, and I. Rolfes, "Determination of the delay spread of an indoor channel measurement campaign in the UHF band," in *Antennas and Propagation Society International Symposium (APSURSI), 2012 IEEE*, 2012.

[4] S. Yano, "Investigating the ultra-wideband indoor wireless channel," in *Vehicular Technology Conference, 2002. VTC Spring 2002. IEEE 55th*, vol. 3, 2002, pp. 1200–1204 vol.3.

[5] J. A. Högbom, "Aperture Synthesis with a Non-Regular Distribution of Interferometer Baselines," *Astronomy and Astrophysics, Supplement*, vol. 15, p. 417, Jun. 1974.

[6] J. Reed, *Introduction to Ultra Wideband Communication Systems, an*, 1st ed. Upper Saddle River, NJ, USA: Prentice Hall Press, 2005.

[7] J. MacQueen, "Some methods for classification and analysis of multivariate observations," Berkeley, Calif., pp. 281–297, 1967. [Online]. Available: http://projecteuclid.org/euclid.bsmsp/1200512992

ISBN 978-3-9812668-6-3